Journal of Radiation Research, Vol. 61, No. 6, 2020, pp. 920–928
doi: 10.1093/jrr/rraa084
Advance Access Publication: 22 September 2020

Application of 3D-print silica bolus for nasal NK/T-cell lymphoma radiation therapy

Guyu Dai[1], Xin Xu[2], Xiaohong Wu[3], Xiaolin Lei[3], Xing Wei[2], Zhibin Li[1], Qing Xiao[1], Renming Zhong[1,†,*] and Sen Bai[1,†]

[1]Department of Radiation Oncology, Cancer Center and State Key Laboratory of Biotherapy, West China Hospital, Sichuan University, Chengdu, China
[2]Department of Obstetrics and Gynecology, West China Second University Hospital, Sichuan University/Key Laboratory of Birth Defects and Related Diseases of Women and Children (Sichuan University), Ministry of Education, Chengdu, China
[3]Department of Oncology, The affiliated Hospital of Panzhihua University, Panzhihua, China
*Corresponding author. Department of Radiotherapy, Division of Radiation Physics, State Key Laboratory of Biotherapy and Cancer Center, West China Hospital, Sichuan University, Chengdu 610041, P.R. China. Tel: +86-28-85422568; E-mail: zrm_100@163.com
[†]These authors contributed equally to this work.
(Received 8 May 2020; revised 28 June 2020; editorial decision 19 August 2020)

ABSTRACT

The aim of the study was to evaluate the clinical feasibility of a 3D-print silica bolus for nasal NK/T-cell lymphoma radiation therapy. Intensity modulated radiotherapy (IMRT) and volumetric modulated arc therapy (VMAT) plans were designed using an anthropomorphic head phantom with a 3D-print silica bolus and other kinds of bolus used clinically, and the surface dose was measured by a metal oxide semiconductor field-effect transistor (MOSFET) dosimeter. Four nasal NK/T patients with or without 3D-print silica bolus were treated and the nose surface dose was measured using a MOSFET dosimeter during the first treatment. Plans for the anthropomorphic head phantom with 3D-print bolus have more uniform dose and higher conformity of the planning target volume (PTV) compared to other boluses; the homogeneity index (HI) and conformity index (CI) of the VMAT plan were 0.0589 and 0.7022, respectively, and the HI and CI of the IMRT plan were 0.0550 and 0.7324, respectively. The MOSFET measurement results showed that the surface dose of the phantom with 3D-print bolus was >180 cGy, and that of patients with 3D-print bolus was higher than patients without bolus. The air gap volume between the 3D-print bolus and the surface of patients was <0.3 cc. The 3D-print silica bolus fitted well on the patient's skin, effectively reducing air gaps between bolus and patient surface. Meanwhile, the 3D-print silica bolus provided patients with higher individuation, and improved the conformity and uniformity of the PTV compared to other kinds of boluses.

Keywords: 3D-print; bolus; nasal NK/T-cell lymphoma; radiotherapy workflow

INTRODUCTION

There is a buildup effect when using high-energy X-rays for radiotherapy [1]. This means that the superficial part of the tumor target area may not receive sufficient dose. Clinically, boluses are often used to produce dose compensation, increasing the dose of superficial tumor targets [2].

Nasal NK/T-cell lymphoma is an independent clinical pathology subtype of lymphoma that is highly relevant to the Epstein–Barr virus [3–5]. The most common symptom in the clinic is nasal congestion [6]. At present, radiotherapy is still the main treatment method for early nasal NK/T-cell lymphoma [7, 8].

Because the target volume of nasal NK/T-cell lymphoma is usually shallow, the bolus is used in clinical treatment to achieve sufficient doses in the shallow target area [9]. At present, the bolus materials commonly used in clinical practice are polymer gel bolus and thermoplastic material bolus [2]. Paraffin is also often used to customize individualized irregular boluses to optimize the dose distribution in the target area. However, the repeatability, durability and homogeneity of these hand-made paraffin boluses may not be easy to guarantee [10].

3D-Print uses special bonding materials such as wax, powdered metal or plastic to print a layer of bonding material to create a 3D object [11]. More and more research uses 3D-print boluses for

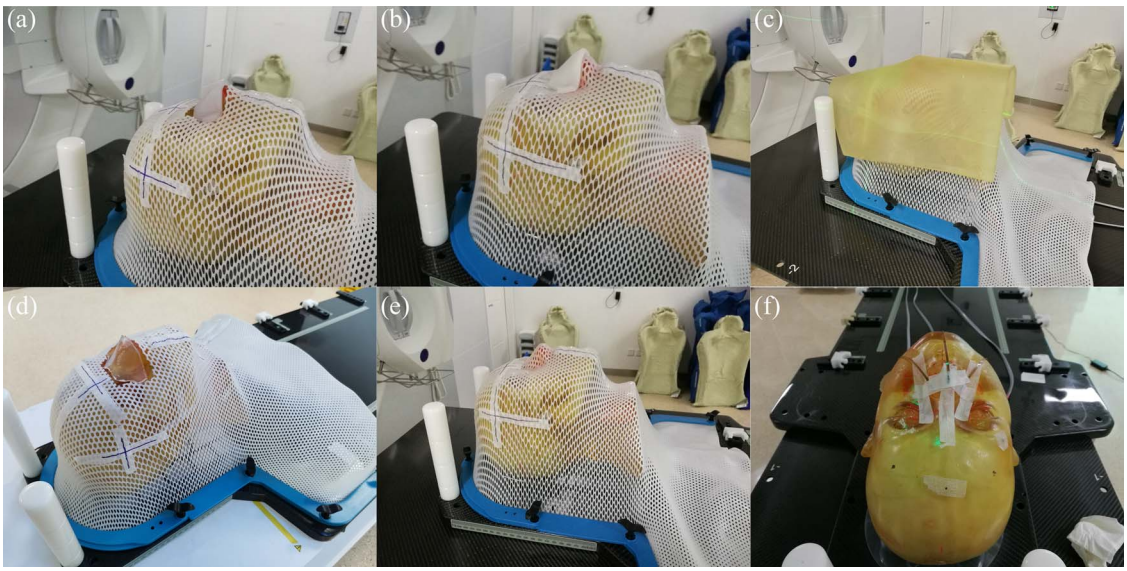

Fig. 1. Measurement setup for surface dose using the anthropomorphic head phantom and various boluses. (a) 3D-print silica bolus; (b) QQ gel bolus; (c) polymer gel bolus; (d) TPE gel bolus; (e) without bolus; (f) using MOSFETs to measure the dose of the head phantom surface, three MOSFET probes were placed at the tip of the nose and on left and right sides of the nose.

radiotherapy [9, 12–14]. However, the majority of research has focused on the workflow of the 3D-print bolus and comparison of different plans [9, 13]. In this study, we chose 3D-print technology to make individualized silica boluses for nasal NK/T patients. We performed both phantom and human experiments and compared both the plan and measured dose for 3D-print bolus with other different clinically used boluses to verify the dose compensation ability of the 3D-print bolus. This study was approved by the Chinese Clinical Trial Registry (ChiCTR1900028011).

MATERIALS AND METHODS

Physical properties verification

3D-Print bolus and three other kinds of clinical boluses were compared (polymer gel bolus, QQ gel bolus and Thermoplastic Elastomer (TPE) gel bolus). The 3D-print bolus is made of silica gel with a density of 1.08 g/cc, shaped according to the shape of the patient's surface, which means that it can fit well with the patient. The polymer gel is a 5 mm thick, 30 cm × 30 cm square material with a density of 0.98 g/cc. When a polymer gel bolus is needed, the therapists will put the whole bolus on the surface of the target area directly; it was often used for breast cancer radiotherapy in our department. The QQ gel bolus is a thermoplastic material with a density of 1.06 g/cc, which becomes soft and easy to shape after heating and is not easily deformed after cooling. A QQ gel bolus is often made after the design of a plan, directly above a thermoplastic mold (Fig. 1b). The TPE gel bolus is a of 5 mm thick, 28 cm × 28 cm square new type material with a density of 0.83 g/cc, which is made of TPE powder and paraffin. When a TPE gel bolus is needed, the bolus is cut to fit the area that needs a bolus. This bolus has a certain viscosity, which means that it closely fits the patient's skin compared to the QQ and polymer gel boluses.

To evaluate the physical characteristics of the boluses, the depth–dose curves of four different kinds of materials were measured with a standard solid water phantom (length: 30 cm, width: 30 cm, height: 10 cm). Four boluses 10 × 10 cm square with a thickness of 5 mm were made of silica gel (3D-print material), polymer gel, QQ gel and TPE gel, respectively. A total of five sets of images were obtained through computed tomography (CT) scans, including the four with different boluses, and one without bolus. The images were transferred to the Raystation treatment planning system (TPS) (version 4.7.5; RaySearch Laboratories AB, Stockholm, Sweden). The 6 MV photon beam, 10 × 10 cm field, Source to Surface Distance (SSD) 100 cm and 100 Monitor Unit (MU) were used for plan design. The dose distributions and depth–dose curves were calculated using Raystation [calculation algorithm: collapsed cone algorithm; grid size: 0.3 × 0.3 × 0.3 cm; linear accelerator: Elekta Versa HD (Elekta, Stockholm, Sweden)] for each plan. Finally, five sets of depth–dose curves at the center of the field were obtained from the calculated dose in Raystation.

Bolus preparation, immobilization and CT scanning for phantom

The anthropomorphic head phantom was immobilized with the thermoplastic mask. For the 3D-print bolus, the anthropomorphic head phantom was scanned with a CT simulator (Siemens Somato, 120 kV, 1 mm thick). We used Mimics (Materialise, Leuven, Belgium) and Magics (Materialise, Leuven, Belgium) to design the 3D-print bolus shell model based on the selected region of interest (ROI), and a SLA 3D Printer (ZRapid Tech, Suzhou, China) was used to print the bolus shell. The shells were filled with silica gel and were removed after the silica gel solidified. After bolus production was completed, the nose part of the thermoplastic mask was cut to prevent the 3D-print silica bolus from being crushed and deformed (Fig. 1a).

For the QQ gel bolus, after immobilizing the head phanthom, the heated and softened QQ gel was placed on the surface of the nose part of the thermoplastic mask, and the QQ gel was cooled to the required shape (Fig. 1b). For the traditional polymer gel bolus, the bolus was placed directly on the surface of the thermoplastic mask when performing the CT simulation or treatment (Fig. 1c). For the TPE gel bolus (Fig. 1d), the same method was used as for the 3D-print silica bolus. The thickness of all boluses was 5 mm, and the size of the 3D-print bolus, QQ gel bolus and TPE gel bolus was kept the same. After immobilization, five sets of CT images of the anthropomorphic head phantom were obtained (including four with bolus and one without bolus).

Radiation therapy plan design for phantom

First, the Clinical Target Volume (CTV) of the head phantom was delineated in TPS by an experienced radiation oncologist, and then expanded 0.5 cm to create a PTV that avoids exceeding the patient's surface. We used the same CTV and PTV for all CT images. A virtual 5 mm bolus was then created (as an Radiotherapy (RT) structure) on CT images of the anthropomorphic head phantom without bolus. The treatment plans were designed using the Raystation TPS (calculation algorithm: collapsed cone algorithm; grid size: 0.3 × 0.3 × 0.3 cm; linear accelerator: Elekta Versa HD) with the prescribed dose for PTV of $D_{95\%} = 6000$ cGy (200 cGy × 30 fractions).

The volumetric modulated arc therapy (VMAT) and intensity modulated radiotherapy (IMRT) plans were designed for the anthropomorphic head phantom with four different boluses, with the virtual bolus and without bolus. VMAT plans were designed with 2 full arc beams, and IMRT plans were designed with 7 beams (P1B1: 204°, P1B2: 256°, P1B3: 308°, P1B4: 0°, P1B5: 52°, P1B6: 104°, P1B7: 156°) and 50 segments. All the plans were optimized with the same conditions. The plan without bolus and the plan with virtual bolus were both based on the CT images of the anthropomorphic head phantom without any bolus. All the plans were normalized to $D_{95\%} = 6000$ cGy.

Comparison of plans with different boluses

The dosimetric parameters D99, D98, D95, D50, D2, D1, D_{mean}, D_{max}, HI, and CI of the PTV were used to compare the RT plans. HI is a homogeneity index related to dose uniformity in the target area. The smaller the HI, the better the homogeneity [15].

$$\mathrm{HI} = \frac{D_2 - D_{98}}{D_{50}}$$

CI is a conformity index used to evaluate the degree of conformity of the target area and the reference isodose surface. The CI value is between 0 and 1; the closer to 1, the higher the conformity [16].

$$\mathrm{CI} = \frac{V_{rx}^2}{V_t \times V_{ri}}$$

V_{rx} indicates the target volume that receives the prescription dose; V_t indicates the volume of the target area; V_{ri} indicates the body volume that receives the prescribed dose.

Phantom dose measurement

MOSFET is a metal oxide semiconductor field-effect transistor, which has a submicron dosimetric volume and allows dosimeters to be used in a confined space like the nasopharyngeal cavity to measure radiation dose [17]. MOSFETs are also very suitable for measuring the surface dose [18]. Therefore, MOSFETs were used to measure the spot dose on the skin surface of the anthropomorphic head phantom.

In this study, a commercial TN-RD-70-W mobileMOSFET system was used. The whole system consisted of a wireless Bluetooth transceiver, five dosimeters (in our study, three standard sensitivity dosimeters were employed), one reader module and a software system (Best Medical, Ottawa, Canada). Each dosimeter was composed of a 1.4 m long cable attached to the length of a thin semiopaque polyimide laminate with a silicon detector. The MOSFET dosimeters were calibrated before measurement. The MOSFET detectors were placed into the grooves in a solid phantom slab (Calibration Jig, TN-RD-57-30), which was designed to ensure the consistency and reproducibility of the MOSFET calibration. Solid water (10 cm thick) was set below the slab as backscatter material and 5 cm thick solid water was placed on top of it. The MOSFETs were irradiated by a 6-MV photon beam produced by an Elekta Versa HD with a field size of 10 × 10 cm^2. The doses measured were then compared with the results of the standard measurements conducted using a 0.6 cm^3 Farmer ionization chamber (IBA-1165). Each measurement was performed at least three times and the average value was taken as the calibration factor. According to the operator's manual from the manufacturer, the linearity error is <1% of the total dose reading; the error resulting from irradiating the dosimeter at any angle is ±2% through 360° of rotation; and in terms of reproducibility, the error is <2% for standard sensitivity mode at a dose level of 200 cGy.

Five sets of plan data were measured (the head phantom with four different boluses and without any bolus). First, the position of the anthropomorphic head phantom was set strictly following the clinical requirements, and three MOSFET probes were placed at the tip of the nose and on the left and right sides of the nose (Fig. 1f). After positioning was completed, a Cone Beam Computed Tomography (CBCT) scan was performed and the image was registered to correct the set-up error. Then the radiation therapy plans were performed on Versa HD. We measured the dose of the surface three times.

Patient dose measurement

Four nasal NK/T-cell lymphoma patients who underwent radiotherapy in our department from November 2019 to December 2019 were enrolled in this study. Three of the patients used a 5 mm 3D-print bolus, and one of the patients did not use bolus because the doctor required that this patient did not need bolus. However, this patient and his doctor agreed to measure the dose of the skin surface during the first treatment, therefore, we collected his dose data. After immobilization and CT scanning were performed, organs at risk were delineated with ABAS (Elekta, Stockholm, Sweden) and then edited by doctors. The CTV and PTV (expand CTV 0.5 cm to create a PTV that avoids exceeding the patient surface) were delineated in TPS by an experienced oncologist. The patients' plans were designed using Raystation (calculation algorithm: collapsed cone algorithm; grid size: 0.3 × 0.3 × 0.3 cm; linear accelerator: Elekta

Versa HD) with two full arcs, and the prescribed dose for PTV was $D_{95\%}$ = 6000 cGy (200 cGy × 30 fractions). All the plans were normalized to $D_{95\%}$ = 6000 cGy. During the first treatment fraction, a CBCT scan was performed and the image was registered to correct the set-up error. Then MOSFETs were used to measure the dose on the surface of the patient's nose during treatment. Three MOSFET probes were placed at the tip of the nose and on the left and right sides of the nose.

Assessment of air gap and comparison of dose

We delineated all air cavities between the bolus and the skin surface on planning CT images for phantom and patients with the help of an automatic CT tool with consistent limits between −1000 and − 800 Hounsfield Unit (HU), and then quantified the total air cavity volume and maximum distance between bolus and surface along the anterior–posterior direction. Due to the partial volume effect and the small size of the air gap between the 3D-print bolus and skin surface, the automatic CT tool did not work in CT images of the 3D-print bolus. Therefore, we manually delineated air cavities on planning CT images for the phantom and patients with 3D-print bolus.

After MOSFET measurement, registration between the CBCT images scanned at the first treatment fraction and planning CT images of the phantom or patient were performed in Raystation. To obtain the mean dose of surface where MOSFETs were placed in the original treatment plans, MOSFET detector areas were delineated on the planning CT images according to CBCT images that contained the spatial location information of the MOSFETs. Then we compared the dose calculated by TPS with the measured dose.

RESULTS

The physical properties of different boluses

The depth–dose curve was calculated at the center of the field, and finally, four depth–dose curves were obtained (Fig. 2c). As shown in Fig. 2(c), when there was no bolus, the surface dose was relatively low, ∼15% of the max dose. 3D-Print bolus, QQ, polymer and TPE gel boluses had similar dose compensation ability, which can increase the dose of superficial tumor targets. The depth of the maximum dose for the 3D-print bolus, QQl, polymer and TPE gel boluses were 1.02, 0.80, 1.04 and 1.08 cm, respectively. However, the depth of the maximum dose was 1.36 cm when there was no bolus on the surface.

Comparison of RT plans

Dosimetric parameters of the PTV are shown in Table 1. In the non-bolus plans, the dose in the PTV was significantly insufficient due to the lack of compensatory effects on the surface of the skin. To achieve a dose of 95% prescription dose (6000 cGy) of the PTV, the overall dose of the target area was increased. For both the IMRT and VMAT plans, the max dose of PTV (6809 and 6639 cGy, respectively) exceeded 110% of the prescribed dose (6600 cGy). Meanwhile, uniformity and conformity were decreased. When there was a bolus on the surface, the max dose of the PTV was reduced, and the uniformity was significantly improved because of the compensatory effects. It can also be seen from the DVH (Fig. 2a and b) that the situation with bolus was better than the case without bolus.

When it comes to HI, CI and other dosimetric parameters (Table 1), the plans with 3D-print bolus had lower HI (0.0589 and 0.0550 for VMAT and IMRT plans, respectively) and higher CI (0.7022 and 0.7324 forVMAT and IMRT plans, respectivley), which meant that these plans have more uniform dose and higher conformity compared to plans with other boluses.

Comparison of dose for anthropomorphic head phantom and patients

The measured phantom dose and TPS calculated dose are shown in Table 2. When there was no bolus on the surface of the phantom, for both the VMAT and IMRT plans, measured average doses were <180 cGy. When it comes to 3D-print bolus, for the VMAT plan, the average measured doses for the left, middle and right sites were 192.3 , 181.7 and 193.3 cGy, respectively, and the difference between measured dose and TPS dose for left, middle and right sites were 4.42, 6.29 and 1.58%, respectively. For the IMRT plan, the average measured dose for the left, middle and right sites were 192.0, 191.3 and 185.3 cGy, respectively, and the differences between measured dose and TPS dose for left, middle and right site were 2.54, 1.39 and 5.02%, respectively.

The dose measured by MOSFETs and the dose calculated by TPS for patients are shown in Table 3. Patient 2 did not use bolus, therefore, the dose of the nose skin was relatively low. A total of 10 of 12 measurements showed difference <10% compared to TPS dose, and 2 measurements showed difference >10%.

Comparison of air gap volume

As is shown in Table 4, when using a 3D-print bolus the maximum distance between bolus and surface along the anterior–posterior direction was <0.4 cm, meanwhile, the air gap volume was <0.3 cc.

DISCUSSION

According to the comparison of the dosimetric parameters of radiotherapy treatment plans for head phantom, the 3D-print bolus can be used to help design better plans with more uniform dose and higher conformity of PTV compared with other kinds of boluses.

The effect of the air gap on surface dose reduction is related to many factors such as field size, incident angle, ray energy and patient characteristics, which brings uncertainty [2]. When using QQ, polymer and TPE gel boluses, the air gap volumes were 1.32 , 9.32 and 0.44 cc, respectively, whereas, the air gap volume was <0.3 cc when using a 3D-print bolus, which meant that the 3D-print bolus can do better in this area compared to other boluses (Fig. 3a, g and h, and Table 4).

The measurement results show that the surface dose of the anthropomorphic head phantom with different kinds of boluses was higher compared to that without bolus, however, there were obvious differences between patients with bolus and patients without bolus. A previous study showed that the mean difference between 48 IMRT MOSFET measured and calculated doses was 3.3% [19]. The mean differences between measured and TPS doses for phantom and patients in our study were 4.19 and 5.12%, respectively. For external beam calculation of multileaf collimator shaped fields in buildup regions the acceptable difference is 20% according to the American Association of Physicists in Medicine Radiation Therapy Task Group 53 [20], and

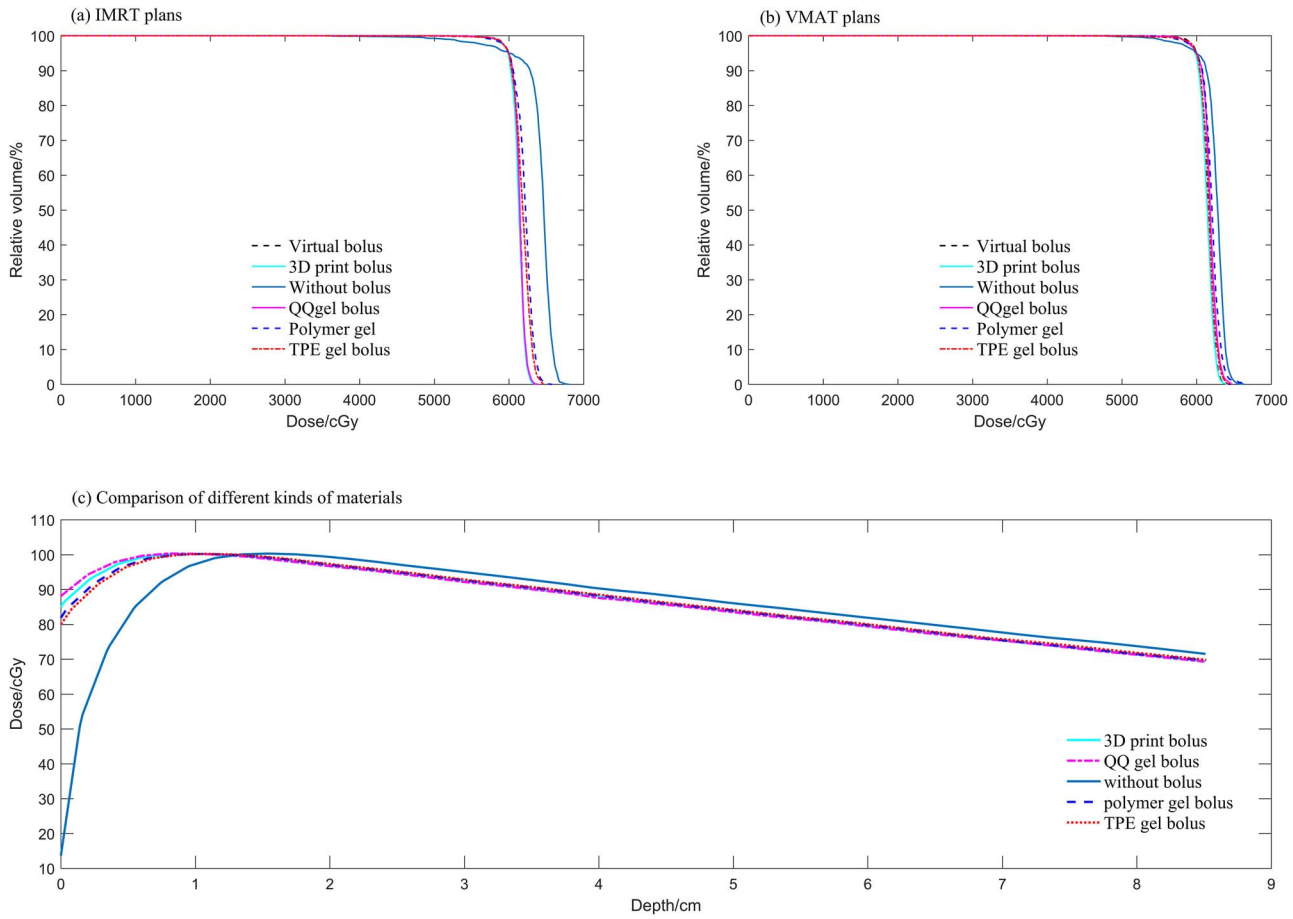

Fig. 2. DVH of the PTV and depth–dose curves for different boluses. (a) DVH of PTV for IMRT plans. (b) DVH of PTV for VMAT plans. (c) TPS-calculated depth–dose curves taken at the center of the field to evaluate the physical properties of different kinds of boluses using the standard solid water phantom.

Table 1. Comparison of VMAT plans and IMRT plans (the unit of D99, D98, D95, D50, D2, D1, D_{mean} and D_{max} is cGy)

Plan	D99	D98	D95	D50	D2	D1	D_{max}	D_{mean}	HI	CI
3D-Print bolus VMAT plan	5897	5946	6000	6145	6308	6329	6419	6141	0.0589	0.7022
3D-Print bolus IMRT plan	5885	5940	6000	6135	6278	6290	6368	6130	0.0550	0.7324
QQ gel bolus VMAT plan	5804	5895	6000	6184	6386	6409	6463	6177	0.0766	0.6337
QQ gel bolus IMRT plan	5817	5901	6000	6168	6311	6320	6511	6156	0.0666	0.6349
Without bolus VMAT plan	5497	5713	6000	6283	6465	6501	6639	6255	0.1197	0.7061
Without bolus IMRT plan	5143	5556	6000	6466	6679	6714	6809	6415	0.1737	0.5992
Virtual bolus VMAT plan	5857	5916	6000	6152	6314	6334	6444	6146	0.0648	0.7314
Virtual bolus IMRT plan	5804	5895	6000	6150	6295	6320	6389	6141	0.0650	0.7488
Polymer gel bolus VMAT plan	5740	5869	6000	6206	6421	6514	6650	6198	0.0889	0.6963
Polymer gel bolus IMRT plan	5760	5900	6000	6222	6418	6449	6561	6207	0.0866	0.6977
TPE gel bolus VMAT plan	5813	5916	6000	6168	6352	6380	6438	6157	0.0706	0.6962
TPE gel bolus IMRT plan	5840	5911	6000	6186	6389	6421	6473	6178	0.0772	0.8029

the difference in our study is <20% except for one measurement for patient 1. Several possible reasons could contribute to this difference. During the measurement process, since the MOSFET detector still had a certain volume, placing the MOSFET detectors on the surface of the anthropomorphic head phantom and patients will change the degree of adhesion of different boluses to the skin surface and change the air

Table 2. Comparison of measured dose and TPS calculated dose of VMAT and IMRT plans for phantoms

		3D-Print bolus		QQ gel bolus		Without bolus		Polymer gel bolus		TPE gel bolus	
		VMAT plan	IMRT plan	VMAT plan	IMRT plan	VMAT plan	IMRT plan	VMAT plan	IMRT plan	VMAT plan	IMRT plan
Left side	First time (cGy)	194	193	188	187	178	178	197	190	178	183
	Second time (cGy)	191	191	187	186	182	181	195	188	179	179
	Third time (cGy)	192	192	186	190	179	180	196	190	180	182
	Average dose (cGy)	192.3	192.0	187.0	187.7	179.7	179.7	196.0	189.3	179.0	181.3
	TPS dose (cGy)	201.2	197.0	195.7	203.3	183.7	179.4	192.6	188.1	196.8	198.0
	Difference	4.42%	2.54%	4.45%	7.67%	2.18%	0.17%	1.77%	0.64%	9.04%	8.43%
Middle	First time (cGy)	182	190	185	190	166	166	191	189	189	197
	Second time (cGy)	181	191	184	188	163	169	187	192	192	200
	Third time (cGy)	182	193	187	190	167	168	188	190	188	198
	Average dose (cGy)	181.7	191.3	185.3	189.3	165.3	167.6	188.7	190.3	189.7	198.3
	TPS dose (cGy)	193.9	194.0	191.8	196.9	166.5	164.4	182.8	181.8	186.3	185.4
	Difference	6.29%	1.39%	3.39%	3.86%	0.72%	1.95%	3.23%	4.68%	1.83%	6.96%
Right side	First time (cGy)	194	186	190	188	177	172	191	190	179	175
	Second time (cGy)	194	185	192	186	178	172	191	187	181	175
	Third time (cGy)	192	185	191	190	179	171	192	188	179	178
	Average dose (cGy)	193.3	185.3	191.0	188.0	178.0	171.7	191.3	188.3	179.7	176.0
	TPS dose (cGy)	196.4	195.1	202.4	199.6	184.7	173.5	183.5	181.7	200.1	199.8
	Difference	1.58%	5.02%	5.63%	5.81%	3.62%	1.03%	4.25%	3.63%	10.19%	11.91%

Table 3. Comparison of measured dose and TPS calculated dose for patients

		Patient 1	Patient 2[a]	Patient 3	Patient 4
Left side	Measured dose (cGy)	150	120	184	197
	TPS calculated dose (cGy)	191.9	127.1	188.6	200.8
	Difference	21.83%	5.59%	2.44%	1.89%
Middle	Measured dose (cGy)	185	118	196	185
	TPS calculated dose (cGy)	195.3	117.6	182.1	197.9
	Difference	5.27%	0.34%	7.63%	6.51%
Right side	Measured dose (cGy)	178	90.5	199	194
	TPS calculated dose (cGy)	183.8	101.3	198.4	188.4
	Difference	3.16%	10.66%	0.30%	2.97%

[a]Patient 2 did not use bolus, therefore, the dose of the nose skin was relatively low.

Table 4. Measured air gap for phantoms and patients

		Air gap volume (cc)	Maximum distance between bolus and surface (cm)
Phantom	3D-Print bolus	0.10	0.30
	QQ gel bolus	1.32	1.02
	Polymer gel bolus	9.32	2.24
	TPE gel bolus	0.44	0.54
Patients	Patient 1	0.28	0.38
	Patient 3	0.24	0.32
	Patient 4	0.09	0.28

gap volume, resulting in some differences between measured dose and dose calculated by TPS. Also, the skin doses measured by MOSFETs could be inaccurate due to the intrinsic buildup in MOSFET detectors [21]. For patient 1, due to the presence of MOSFET detectors, the air gap between bolus and skin increased, especially on the left side of the nose, which resulted in a relatively low dose.

At present, there are still many kinds of tumor that may need bolus to produce dose compensation, such as nasal NK/T-cell lymphoma and breast cancer. However, the QQ gel bolus was made after the physicist had completed the design of the radiotherapy plan, which could cause several problems. First, the physicist designed the plan after adding the virtual bolus to the TPS, and the virtual bolus will differ from the actual clinically used boluses in terms of shape, density and dose compensation ability. Secondly, the clinically used bolus was made above the head and neck thermoplastic mold, which means there was an air gap between the QQ gel bolus and the patient's skin (Fig. 3b). However, there was no gap between the virtual bolus added in the actual clinical design plan and the patient's skin surface, which will result in a certain degree of dose difference.

With regard to the polymer gel bolus, this bolus was used after the plan had been designed, which still caused a difference between plan design and actual treatment. Besides, polymer gel boluses are often very big, and when using them, therapists just put them on the surface of a patient, which will increase the dose for other tissues. In addition, using a polymer gel bolus can also cause a big air gap between the bolus and surface of the skin (Fig. 3c). Kong *et al.* [9] also compared polymer gel bolus with the 3D-print bolus, and the results show that V95%, HI and CI of the 3D-print bolus were better than those of the polymer gel bolus. Therefore, we believe that a polymer gel bolus is not suitable for nasal NK/T-cell lymphoma radiotherapy.

The TPE gel bolus had a certain viscosity, which meant that compared with other traditional boluses, it fitted tightly with the patient's skin. Because the manufacturer did not produce the bolus according to the patients' actual situation, there was still an air gap between the bolus and the skin (Fig. 3e).

If the 3D-print silica bolus is used, the whole radiotherapy workflow has certain changes (Fig. 4). After the oncologist gave the patient a prescription for radiation therapy, we first scanned the surface of the skin of the patient and performed production of the bolus, followed by immobilization and CT scanning. The physicist designed the plan based on the CT images containing the 3D-print bolus information. Finally, the patient began treatment after receiving a virtual simulation. There will be several benefits if we use a 3D-print bolus. First, the 3D-print bolus was made after scanning the surface of patients, and the material used was silica gel which is softer than QQ gel and polymer gel, which meant that the 3D-print bolus fitted better with the patient's skin surface than QQ, polymer and TPE gel boluses (Fig. 3). Second, we performed the CT scanning after the 3D-print bolus was completed, which meant that as the CT image contains 3D-print bolus information, it was no longer necessary to add a virtual bolus and the designed radiotherapy plan was closer to the clinical treatment

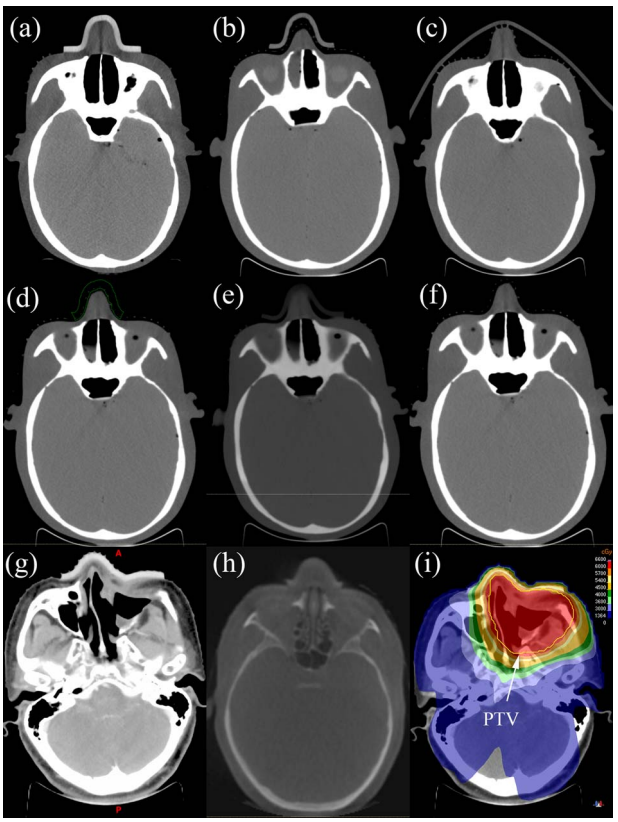

Fig. 3. The CT and CBCT images of phantom and patients for different boluses. (a–g and i) are CT images, and (h) is a CBCT image. (a) 3D-Print silica bolus; (b) QQ gel bolus; (c) polymer gel bolus; (d) virtual bolus; (e) TPE gel bolus; (f) without bolus; (g h) CT and CBCT images for two different patients who use a 3D-print silica bolus. (a– f) CT images for the phantom. (i) Dose distribution of patient 4 with a 3D-print silica bolus.

situation. Third, patients will feel more comfortable when using soft silica material.

3D-Print silica bolus production takes 4–6 h and it costs about 1000 CNY, which means that the patient's treatment time is not extended and the cost is acceptable for patients. If we make personalized 3D-print boluses for patients, there is almost no air gap between bolus and surface which means that the bolus can perform dose compensation better, in addition the radiation therapy plan design will be more accurate and of better quality compared to other boluses. Therefore, we believe that 3D-print bolus is clinically feasible.

CONCLUSION

The 3D-print silica bolus can provide patients with individualized treatment for nasal NK/T-cell lymphoma radiotherapy. Compared with QQ, polymer or TPE gel boluses it can meet the clinical needs while improving the conformity and uniformity of the target area, and reduce the air gap between surface and bolus. Additionally, the radiotherapy workflow was optimized by using a 3D-print bolus.

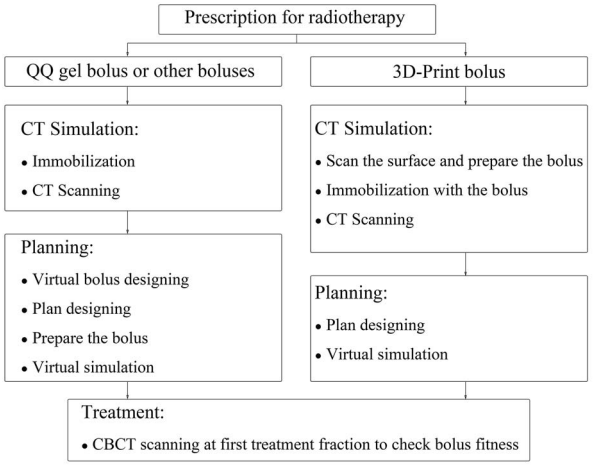

Fig. 4. Radiotherapy workflow of patients who use QQ gel bolus or 3D-print silica bolus.

FUNDING

This work was supported by the Science and Technology Support Program of Sichuan province, China (Grant number.2016FZ0086).

CONFLICT OF INTEREST

The authors state that there are no conflicts of interest.

REFERENCES

1. Podgoršak EB, International Atomic Energy Agency. *Radiation oncology physics: a handbook for teachers and students*. Vienna: International Atomic Energy Agency, 2005.
2. Vyas V, Palmer L, Mudge R et al. On bolus for megavoltage photon and electron radiation therapy. *Med Dosim* 2013;38:268–73.
3. Chen H, Zhang Y, Jiang Z et al. A case report of NK-cell lymphoproliferative disease with a wide involvement of digestive tract develop into Epstein-Barr virus associated NK/T cell lymphoma in an immunocompetent patient. *Medicine (Baltimore)* 2016;95:e3176.
4. Yamaguchi M, Suzuki R, Miyazaki K et al. Improved prognosis of extranodal NK/T cell lymphoma, nasal type of nasal origin but not extranasal origin. *Ann Hematol* 2019;98:1647–55.
5. Huang MJ, Jiang Y, Liu WP et al. Early or up-front radiotherapy improved survival of localized extranodal NK/T-cell lymphoma, nasal-type in the upper aerodigestive tract. *Int J Radiat Oncol Biol Phys* 2008;70:166–74.
6. Termuhlen AM. Natural killer/T-cell lymphomas in pediatric and adolescent patients. *Clin Adv Hematol Oncol* 2017;15:200–9.
7. Li YX, Liu QF, Wang WH et al. Failure patterns and clinical implications in early stage nasal natural killer/T-cell lymphoma treated with primary radiotherapy. *Cancer* 2011;117:5203–11.
8. Qi SN, Xu LM, Yuan ZY et al. Effect of primary tumor invasion on treatment and survival in extranodal nasal-type NK/T-cell lymphoma in the modern chemotherapy era: A multicenter study from the China lymphoma collaborative group (CLCG). *Leuk Lymphoma* 2019;60:2669–78.

9. Kong Y, Yan T, Sun Y et al. A dosimetric study on the use of 3D-printed customized boluses in photon therapy: A hydrogel and silica gel study. *J Appl Clin Med Phys* 2019;20:348–55.
10. Lukowiak M, Jezierska K, Boehlke M et al. Utilization of a 3D printer to fabricate boluses used for electron therapy of skin lesions of the eye canthi. *J Appl Clin Med Phys* 2017;18:76–81.
11. Lim KH, Loo ZY, Goldie SJ et al. Use of 3D printed models in medical education: A randomized control trial comparing 3D prints versus cadaveric materials for learning external cardiac anatomy. *Anat Sci Educ* 2016;9:213–21.
12. Canters RA, Lips IM, Wendling M et al. Clinical implementation of 3D printing in the construction of patient specific bolus for electron beam radiotherapy for non-melanoma skin cancer. *Radiother Oncol* 2016;121:148–53.
13. Su S, Moran K, Robar JL. Design and production of 3D printed bolus for electron radiation therapy. *J Appl Clin Med Phys* 2014;15:4831.
14. Baltz GC, Chi PM, Wong PF et al. Development and validation of a 3D-printed bolus cap for total scalp irradiation. *J Appl Clin Med Phys* 2019;20:89–96.
15. Kataria T, Sharma K, Subramani V et al. Homogeneity index: An objective tool for assessment of conformal radiation treatments. *J Med Phys* 2012;37:207–13.
16. Barbiero S, Rink A, Matteucci F et al. Single-fraction flattening filter-free volumetric modulated arc therapy for lung cancer: Dosimetric results and comparison with flattened beams technique. *Med Dosim* 2016;41:334–8.
17. Luo GW, Qi ZY, Deng XW et al. Investigation of a pulsed current annealing method in reusing MOSFET dosimeters for in vivo IMRT dosimetry. *Med Phys* 2014;41:051710.
18. Sun W, Wang B, Qiu B et al. Assessment of female breast dose for thoracic cone-beam CT using MOSFET dosimeters. *Oncotarget* 2017;8:20179–86.
19. Qi ZY, Deng XW, Huang SM et al. Real-time in vivo dosimetry with MOSFET detectors in serial tomotherapy for head and neck cancer patients. *Int J Radiat Oncol Biol Phys* 2011;80:1581–8.
20. Fraass B, Doppke K, Hunt M et al. American Association of Physicists in Medicine radiation therapy committee task group 53: Quality assurance for clinical radiotherapy treatment planning. *Med Phys* 1998;25:1773–829.
21. Xiang HF, Song JS, Chin DW et al. Build-up and surface dose measurements on phantoms using micro-MOSFET in 6 and 10 MV x-ray beams and comparisons with Monte Carlo calculations. *Med Phys* 2007;34:1266–73.